Imaging and Spectroscopy of the Au Nanoclusters in the YSZ Films by Ballistic Electron/Hole Emission Microscopy

D. O. Filatov*, D. V. Guseinov*, I. A. Antonov*, O. N. Gorshkov*, A. I. Bobrov** and D. A. Pavlov**

* Physical Technical Research Institute, N. I. Lobachevskii University of Nizhny Novgorod
23 Gagarin Ave., Nizhny Novgorod 603950, Russia, filatov@phys.unn.ru
** Department of Physics, N. I. Lobachevskii University of Nizhny Novgorod
23 Gagarin Ave., Nizhny Novgorod 603950, Russia

ABSTRACT

We report on application of Ballistic Electron/Hole Emission Microscopy (BEEM/BHEM) to imaging and spectroscopy of Au nanoclusters (NCs) in the ultrathin ($\approx$ 6 nm) yttria stabilized zirconia (YSZ) films on Si grown by Magnetron Sputtering. Cross-sectional Transmission Electron Microscopy (TEM) revealed spherical Au NCs of 1.5 to 3.5 nm in diameter arranged in a single sheet inside the YSZ film. The BEEM images demonstrated the spots of increased collector current of 1 to 2.5 nm in size related to the ballistic electron tunnelling via the Au NCs. BEEM spectra of the NCs demonstrated the stepwise features attributed to the quantum confined states in the Au NCs. The estimate of the NC diameter by the best fit between the measured quantum state energies and the ones calculated for a spherical quantum dot model yielded 3 ± 4 nm that is consistent with the TEM data.

Keywords: metal nanoclusters, imaging, specroscopy

1 INTRODUCTION

Recently metal nanoclusters (NCs) embedded into the ultrathin ($\sim$ 10 nm) dielectric films attracted much attention because of their potential application in the floating gate Metal-Oxide-Semiconductor Field Effect Transistors (MOSFETs), which are promising for the non-volatile memory devices [1]. Transmission Electron Microscopy (TEM) is applied for structural characterization of the metal NCs in the dielectric matrices usually [2]. In the present study we have applied Ballistic Electron/Hole Emission Microscopy (BEEM/BHEM) to imaging and spectroscopy of the electron states in the Au NCs in the ultrathin ($\approx$ 6 nm) yttria stabilized zirconia (YSZ) films on Si. Such films are promising for the resistive non-volatile memory applications [3]. Earlier, BEEM/BESS has been proven to be a powerful tool for measuring the energy barrier heights in the MOS stacks and for imaging and spectroscopy of the semiconductor quantum dots (QDs) [4]. In the present work we have demonstrated the capabilities of BEEM/BHEM in imaging the metal NCs embedded into the ultrathin dielectric films and in the spectroscopy of the quantum confined electron states in the ultrafine metal NCs.

2 EXPERIMENT

The YSZ films with Y_2O_3 molar fraction of ≈ 0.12 were deposited by Magnetron Sputtering at the substrate temperature 300°C using Torr International 1G2-2G1 setup. The nanocomposite films for BEEM/BEES investigations consisting of the $\approx$ 3 nm thick underlying YSZ layers, the $\approx$ 1 nm thick Au layers, and the $\approx$ 3 nm thick cladding YSZ layers were deposited onto the n-Si(001) substrates with the electron concentration $n \approx 2.5 \times 10^{15}$ cm^{-3}. and annealed in air at 800°C for 2 min. Also, the YSZ/Si(001) films $\approx$ 6 nm in thickness were fabricated to serve as the reference samples. Finally, the $\approx$ 5 nm thick Au base electrodes were deposited onto the YSZ surfaces.

The structure of the YSZ:nc-Au films was examined by Cross-sectional High Resolution (HR) TEM using Jeol JEM-2100/F instrument. The YSZ:nc-Au films for TEM investigations were deposited on the Au/Si substrates, the thicknesses of both underlying and cladding YSZ layers were selected to be $\approx$ 20 nm in order to make the cross section preparation easier. The Au layer thickness, annealing temperature and time were the same as in the samples for the BEEM measurements.

The BEEM/BHEM experiments were carried out in ambient air at 300K using a home-made setup based on NT-MDT Solver Pro atomic force microscope (AFM). The scanning sample scheme was utilized. The first stage collector current preamplifier (the current voltage converter) was built inside the sample holder mounted onto the tube piezoscanner. The ground contacts to the Au base electrodes were provided by a bronze spring. The home-made scanning tunnelling microscope (STM) head utilized a tip-biased tip current preamplifier form NT-MDT Smena EC electrochemical AFM. The STM probes were made from a tungsten wire sharpened by electrochemical etching.

The BEEM/BHEM images were recorded in the constant current mode at constant gap voltage V_g applied between the STM tip and the Au base electrodes. The BEEM/BHEM spectra were measured with the tip current feedback switched on. The differential BEEM/BHEM spectra dI_c/dV_g where I_c is the collector current were calculated from the measured $I_c(V_g)$ curves by numerical differentiation with nonlinear smoothing.

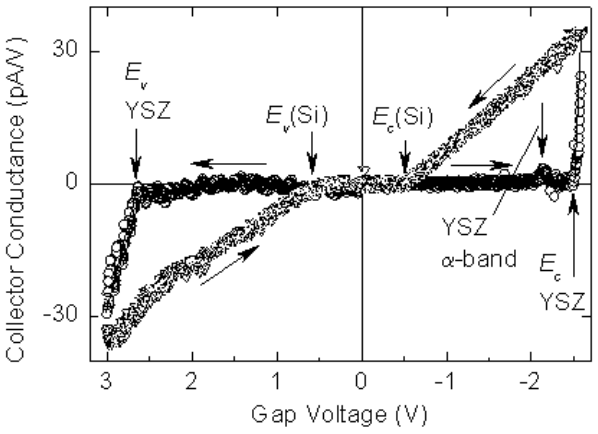

Figure 1: A cyclic BEEM/BHEM spectrum (300K) of an Au(5 nm)/YSZ(6 nm)/n-Si stack. The arrows denote the directions of the gap voltage V_g sweep.

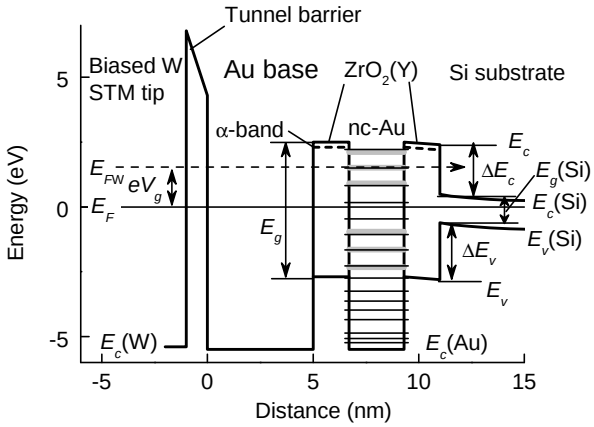

Figure 2: Band diagram of a contact of a STM tip to an Au(5 nm)/YSZ(3 nm)/nc-Au/YSZ(3 nm)/n-Si stack and the schematic of the ballistic electron transport via a quantum confined energy level in the Au NC in the BEEM measurements. The measured (bold grey lines) energy levels in the Au NC and the calculated ones for $D_c = 3.6$ nm (solid lines) are shown.

3 RESULTS AND DISCUSSION

The cyclic BEEM/BHEM spectra of the Au/YSZ/Si reference sample (Fig. 1) demonstrated an expressed hysteresis. The spectrum measured at the forward V_g sweep demonstrated a threshold at $V_g = (-2.5 \pm 0.1)$ V related to the YSZ conduction band edge E_c (Fig. 2). Also, a peak at $V_t \approx -2.15$ V attributed to the electron transport via the oxygen vacancy band (α-band) in YSZ lying at $\approx E_c - 0.3$ eV [5] has been observed. The hysteresis in the BEEM spectrum was attributed to the damage of the sample by the increased setpoint tip current $I_t = 10$ nA at $V_g < -2.5$ V so that a pinhole has been burned through both the Au base and the YSZ layer. Ballistic Electron Emission Spectroscopy (BEES) measurements in a pinhole appeared to be a powerful tool for the investigations of the inner barriers in the complex structures [6]. In the present study, a threshold at $V_g = (-0.5 \pm 0.1)$ V has been observed in the spectrum recorded at the backward V_g sweep (Fig. 1). This threshold was related to the conduction band edge in the Si substrate at the YSZ/Si interface E_c(Si). Because of a small size of the pinhole (several nm) the surface potential at the Si surface inside the pinhole could be assumed to be equal to the one at the YSZ/Si interface outside the hole [6]. The conduction band edge in the quasi neutral layer of the Si substrate E_{c0}(Si) relative to the Fermi level energy for non-degenerated n-Si could be calculated according to a well known formula [7]

$$E_{c0}(\mathrm{Si}) - E_F = \frac{kT}{e} \ln\left(\frac{N_c}{n}\right) \quad (1)$$

where k is Boltzmann constant, T is the temperature, and N_c is the effective density of states in the conduction band of Si. For $n = 2.5 \times 10^{15}$ cm^{-3} at 300K one gets $E_{c0}(\mathrm{Si}) - E_F \approx 0.25$ eV. So far, the potential barrier height at the YSZ/Si interface $\Delta\varphi = E_c(\mathrm{Si}) - E_{c0}(\mathrm{Si}) \approx 0.25$ eV. Now, the conduction band offset at the YSZ/Si interface can be found taking into account the potential drop across the YSZ film from the condition of the electric flux density continuity at the YSZ/Si interface:

$$\varepsilon_{\mathrm{YSZ}} F_{\mathrm{YSZ}} = \varepsilon_{\mathrm{Si}} F_{\mathrm{Si}} \quad (2)$$

where F_{YSZ} and $\varepsilon_{\mathrm{YSZ}}$ are the electric field strength and the dielectric constant for YSZ, respectively; F_{Si} and $\varepsilon_{\mathrm{Si}}$ are the respective quantities for Si. Assuming $\varepsilon_{\mathrm{YSZ}} = 25$ [5] and $\varepsilon_{\mathrm{Si}} = 11.7$ [7] one gets $\Delta E_c = 1.9 \pm 0.1$ eV.

Similar hysteresis has been observed in the spectra recorded at the positive tip bias with respect to the Au base, i.e. in the Ballistic Hole Emission Spectroscopy (BHES) mode (Fig. 1). A threshold at $V_g = (2.7 \pm 0.1)$ V in the spectrum measured at the forward V_g sweep has been attributed to the YSZ valence band edge E_v (Fig. 2). Note that according to this result, the Fermi energy in Au base $E_F - E_c(\mathrm{Au}) \approx 5.5$ eV [8] is higher than the energy spacing between the Fermi level in the Au base E_F and the valence band edge in YSZ $E_F - E_v \approx 2.7$ V (Fig. 2). This factor makes the observation of the threshold related to the YSZ valence band edge in the BHEM spectra possible. The threshold at $V_g = (0.6 \pm 0.1)$ eV observed at the backward V_g sweep was related to the valence band edge in Si at the YSZ/Si interface E_v(Si). From the above data, the valence band offset at the YSZ/Si interface $\Delta E_v \approx 2.1$ eV can be evaluated. Note that the resulting energy gap for Si E_g(Si) = 0.5 eV + 0.6 eV $\approx$ 1.1 eV is consistent with the ref-

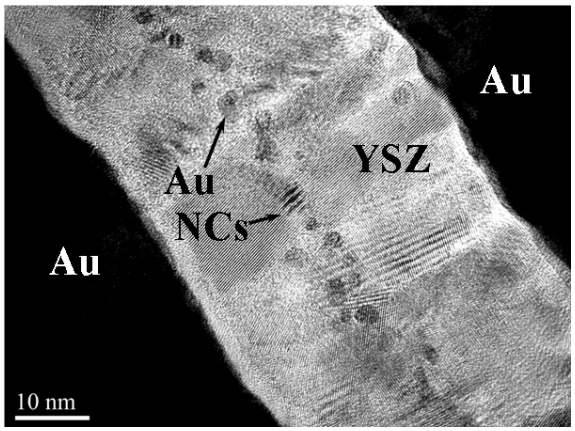

Figure 3: High resolution cross-sectional TEM image of an Au/YSZ(20 nm)/nc-Au/YSZ(20 nm)/Au/Si stack with the Au NCs formed in the same conditions as in the samples for BEEM/BHEM investigations (annealing temperature $T_A = 800$°C; annealing time $t_A = 2$ min). The accelerating voltage $U_A = 180$ kV.

erence data [7] that confirms the accuracy of the calculations above. On the other hand, the BEES/BHES measurements yielded the YSZ energy gap $E_g \approx 5.2$ eV, which appears to be lower than the respective value obtained by optical transmission spectroscopy (5.6 ± 0.1 eV at 300K) [9]. This disagreement could probably attributed to residual strain in the YSZ film originating from the difference in the thermal expansion coefficients for Si and YSZ ($\approx 2.6 \cdot 10^{-6}$ K^{-1} [7] and $\approx 8 \cdot 10^{-6}$ K^{-1} [5], respectively).

Thus, applying the combination of BEES and BHES allowed measuring all energy gaps in Au/YSZ/Si MOS stack necessary to calculate a complete band diagram of the structure (Fig. 2). These energy gaps obtained have been used further to calculate the quantum confined level energies in the Au NCs in the YSZ matrix.

The cross-sectional HR TEM studies performed on the Au/YSZ(20 nm)/nc-Au/YSZ(20 nm)/Au/Si stack (Fig. 3) revealed nearly spherical Au NCs with the diameter $D_c = (2.5 \pm 1)$ nm to be arranged in a single sheet between the YSZ layers almost strictly. It is worth noting that cross sectional HR TEM with atomic resolution demonstrates clearly both underlying and cladding YSZ layers to be the nanocrystalline ones so that the nanocrystal size was approximately equal to the whole underlying (cladding) YSZ layer thickness. At the same time, X-ray diffraction patterns from the YSZ/Si films deposited in the same conditions demonstrated a number of broad halos typical for the the amorphous materials [10]. Taking into account the TEM data, these diffraction patterns could be interpreted to be a result of the Scherrer's reflection broadening due to small sizes of the YSZ nanocrystals, which the films consisted of.

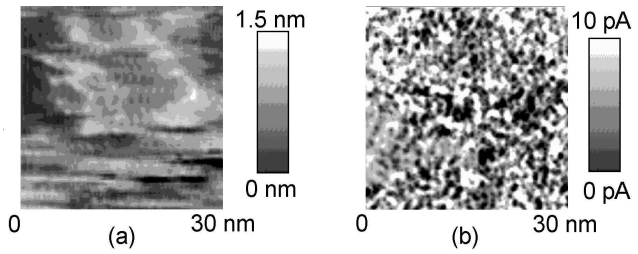

[b]

Figure 4: STM topography (a) and BEEM (b) images of an Au(5 nm)/YSZ(3 nm)/nc-Au/YSZ(3 nm)/n-Si stack measured at the tip current $I_t = 10$ nA and the gap voltage $V_g = 2$ V.

The BEEM image of the Au(5 nm)/YSZ(3 nm)/nc-Au/YSZ(3 nm)/n-Si stack [Fig. 4(b)] demonstrated the spots of increased collector current I_c of 1 to 2.5 nm in size related to the ballistic electron tunnelling via the Au NCs as shown in Fig. 2. The surface density of the spots in the BEEM image in Fig. 4(a) $N_s \approx 3.4 \cdot 10^{13}$ cm^{-2} that is of the same order of magnitude as the NC density estimated form the TEM image in Fig. 3 ($N_s \approx 1.8 \cdot 10^{13}$ cm^{-2}).

The BEEM spectra dI_c/dV_g of the Au(5 nm)/YSZ(3 nm)/nc-Au/YSZ(3 nm)/n-Si stack recorded in the spots of increased collector current I_c (corresponding to the Au NCs) and between these ones are presented in Fig. 5. The BEEM spectra measured between the Au NCs exhibited the thresholds at $V_g \approx -2.4$ V and the peaks at $V_g \approx -2.1$ V (Fig. 5) attributed to the conduction band edge in YSZ E_c and to the oxygen vacancy α-band in YSZ, respectively as in the BEEM spectra of the reference Au(5 nm)/YSZ(6 nm)/n-Si stack (Fig. 1). The BEEM spectra measured on the Au NCs demonstrated the stepwise features attributed to the quantum confined states in the Au NCs. The theory predicts the peaks in the d^2I_c/dV_g^2 spectra of the QDs corresponding to the quantum confined energy levels in the zero-dimensional (0D) objects [11]. Accordingly, the steps should be observed in the dI_c/dV_g spectra of the QDs as it has been observed in the BEEM spectra of the Au NCs in YSZ films in the present study (Fig. 5).

The BHEM spectrum of the Au(5 nm)/YSZ(3 nm)/nc-Au/YSZ(3 nm)/n-Si stack measured between the Au NCs (Fig. 5) exhibited a threshold at $V_g \approx 2.6$ V attributed to the YSZ valence band edge E_v, as in the reference Au/YSZ/Si sample (Fig. 1). The spectra measured on the Au NCs demonstrated the stepwise features similar to the ones in the BEEM spectra. These features were attributed to the ballistic electron tunnelling from the Si valence band states into the free states above Fermi level in the STM tip material via the quantum confined states in the Au NCs lying between the valence band edge in Si E_v(Si) and the valence band edge in YSZ

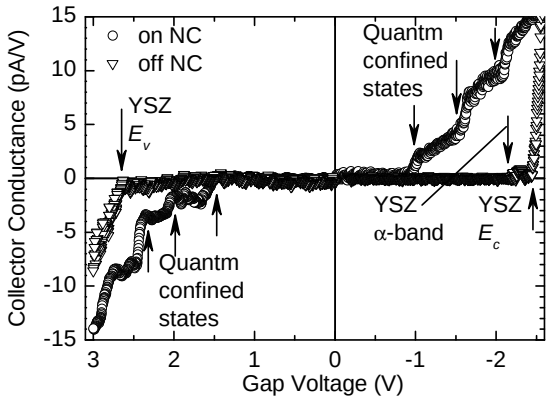

Figure 5: BEEM/BHEM spectra (300K) of an Au(5 nm)/YSZ(3 nm)/nc-Au/YSZ(3 nm)/n-Si stack. The arrows denote the quantum confined states in the Au NC.

E_v (Fig. 2) that could be also described in terms of the ballistic hole injection from the STM tip into the valence band states in the Si substrate. Note that according to the BHES data, the bottom of the potential well of Au NCs in YSZ matrix $E_c(\mathrm{Au}) \approx -5.5$ eV appears to be lower than the YSZ valence band edge $E_v \approx -2.7$ eV, i. e. the Au QDs in the YSZ matrix appeared to be the ones of type II.

Using the data on the energy gaps in the Au/YSZ/n-Si(001) stacks provided by BEES/BHES, the size quantization spectrum for the electrons in the Au NCs has been calculated as a function of the NC diameter D_c according to the model of a spherical QD with a finite potential well height in the effective mass approximation [12]. Along with a standard boundary conditions for the continuity of the radial parts of the envelope wavefunctions of the bound electron states $\chi(r)$ at the YSZ/Au interface: $\chi_{\mathrm{Au}} = \chi_{\mathrm{YSZ}}$, Bastard's boundary conditions were imposed onto the envelope derivatives:

$$m_{\mathrm{Au}} \frac{\partial \chi_{\mathrm{Au}}}{\partial r} = m_{\mathrm{YSZ}} \frac{\partial \chi_{\mathrm{YSZ}}}{\partial r} \qquad (3)$$

where m_{Au} and m_{YSZ} are the effective electron masses in Au and YSZ, respectively. We assumed $m_{\mathrm{YSZ}} = 0.7$ [13] and $m_{\mathrm{Au}} = 1$. The spin-orbit interaction as well as Coulomb one for the electrons inside the QDs were neglected. An example of the size quantization energy spectrum in the Au NC calculated for $D_c = 3.6$ nm is presented in Fig. 2. An estimate of D_c by the best fit between the quantum confined state energies determined from the BEEM/ BHEM spectra and the calculated ones yielded $D_c = 3.5 \pm 0.5$ nm. Taking into account that the effective mass approximation is rather rough for the Au NCs in YSZ matrix, the agreement of this estimate with the TEM data could be considered to be satisfactory.

4 CONCLUSIONS

The results of present study demonstrate the capabilities of BEEM/BHEM in imaging the Au NCs inside the YSZ films and in measuring the size quantization energies of electrons in small Au NCs directly. These results open the prospects for wide application of BEEM/BHEM for characterization of the ultrathin dielectric films with metal NCs in both research and production.

5 ACKNOWLEDGEMENTS

The authors gratefully acknowledge the financial support from Ministry of Education and Science, Russian Federation within the framework of State Research Program, Task 2014/134 (Project No. 2591).

REFERENCES

[1] E. Coplin and U. Simon, "Metal Nanoclusters in Catalysis and Materials Science: The Issue of Size Control," Elsevier, 107, 2008.

[2] V. P. Zhdanov and B. Kasemo, Surf. Sci. Rep. 39, 25, 2000.

[3] W. Guan , S. Long, R. Jia and M. Liu, Appl. Phys. Lett. 91, 062111, 2007.

[4] V. Narayanamurti and M. Kozhevnikov, Phys. Rep. 349, 447, 2001.

[5] H. A. Abbas, "Stabilized Zirconia for Solid Oxide Fuel Cells or Oxygen Sensors: Characterization of Structural and Electrical Properties of Zirconia Doped with Some Oxides," LAP Lambert Academic, 2012.

[6] A. Bauer and R. Ludeke, J. Vac. Sci. Technol. B 12, 2667, 1994.

[7] K. Seeger, "Semiconductor Physics: An Introduction (Advanced Texts in Physics)," Springer, 2004.

[8] G. Ozdemir and S. Maghsoodloo, "Smithells Metals Reference Book," Elsevier, 39, 2004.

[9] S. Heiroth, R. Ghisleni, T. Lippert, J. Michler and A. Wokaun, Acta Mater. 59, 2330, 2011.

[10] O. N. Gorshkov, D. A. Pavlov, V. N. Trushin, I. N. Antonov, M. E. Shenina, A. I. Bobrov, A. S. Markelov, A. Yu. Dudin, A. P. Kasatkin, Tech. Phys. Lett. 38, 185, 2012.

[11] J. Walachova, J. Zelinka, V. Malina, J. Vanis, F. Sroubek, J. Pangrac, K. Melichar and E. Hulicius, Appl. Phys. Lett. 92, 012101, 2008.

[12] A. Messiah, "Quantum Mechanics," North Holland 1, 78, 1967.

[13] T. V. Perevalov, A. V. Shaposhnikov, K. A. Nazyrov, D. V. Gritsenko, V. A. Gritsenko amd V. M. Taplin, "Defects in HIgh-k Gate Dielectric Stacks: Nano-Electronic Semiconductor Devices," Springer, 430, 2006.